Methods to locate Saddle Points in Complex Landscapes

Silvia Bonfanti[a,b,c] and Walter Kob[c]

[a] Dipartimento di Scienza ed Alta Tecnologia, Università dell'Insubria, Via Valleggio 11, 22100 Como, Italy
[b] Department of Physics, University of Milano, via Celoria 16, 20133 Milano, Italy
[c] Laboratoire Charles Coulomb, Université de Montpellier and CNRS, UMR 5221, 34095 Montpellier, France

We present a class of simple algorithms that allows to find the reaction path in systems with a complex potential energy landscape. The approach does not need any knowledge on the product state and does not require the calculation of any second derivatives. The underlying idea is to use two nearby points in configuration space to locate the path of slowest ascent. By introducing a weak noise term, the algorithm is able to find even low-lying saddle points that are not reachable by means of a slowest ascent path. Since the algorithm makes only use of the value of the potential and its gradient, the computational effort to find saddles is linear in the number of degrees of freedom, if the potential is short-ranged. We test the performance of the algorithm for two potential energy landscapes. For the Müller-Brown surface we find that the algorithm always finds the correct saddle point. For the modified Müller-Brown surface, which has a saddle point that is not reachable by means of a slowest ascent path, the algorithm is still able to find this saddle point with high probability.

I. INTRODUCTION

Many static and dynamics properties of complex many body systems can be understood using the concept of the potential energy landscape (PEL), i.e. the hypersurface defined by the interaction potential $V(\{\mathbf{r}_i\})$ between the particles as a function of their coordinates $\mathbf{r}_i$, $i = 1, 2...N$, with N the total number of particles in the system. Examples for which such an approach has been found to be useful include chemical reactions (reaction path), atomic diffusion (overcoming the local barriers), but also systems that involve many particles such as proteins (folding pathway) and glasses (nature of the relaxation dynamics)[1]. To understand the static and dynamic properties of such systems one usually relies on the fact that at low temperatures one has a separation of time scales: On short times the system is vibrating around a local minimum of the PEL while on longer time scales it hops over a local barrier. Thus the knowledge of the distribution of the location and height of the local minima allows to understand many of the static properties of the system: The shape of the local minima gives information about the vibrational properties, and the height of the barrier that connects neighboring minima allows to make a coarse grained description of the dynamics of the system[2]. Finally we mention that these details of the PEL are also needed to determine some of the properties of glasses lt ow temperature since, e.g., a realistic description of the tunneling processes depends in a crucial manner on the geometry of the PEL[3].

It is often found that the number of such local minima increases exponentially with the number of degrees of freedom of the system, in particular if the system of interest is complex such as it is the case with proteins or glasses[4]. Thus the PEL is very rugged and it is therefore a formidable task to find the location of *all* these minima. However, using specialized algorithms it is indeed possible to obtain this information on relatively simple systems that have, typically, less than hundred particles[5–9].

Despite these approaches it is at present impossible to determine numerically the complete landscape of a complex bulk system that has, say, $\mathcal{O}(10^3)$ particles.

Notwithstanding this impossibility, it is not very difficult to find at least a large number of local minima, since algorithms like the steepest descent procedure allow to efficiently determine for a given starting point in configuration space the nearest local minimum[10], a configuration that in the following we will refer to as "inherent structure" (IS)[11]. Such an approach has allowed, e.g., to obtain interesting properties of the PEL in glass-forming systems[7,11–20].

Much more difficult is the location of the saddle points (SP) that connect neighboring minima, information that is needed to determine the reaction path and the corresponding energy barrier. Roughly speaking one can identify three approaches to find such saddle points:

1. In the case that one knows two minima that are neighbors one can use simple and efficient algorithms that are able to find the corresponding saddle point with a modest numerical effort. A typical example for such a method is the so-called "nudged elastic band" which is basically a minimization of the forces acting on a one dimensional elastic band that connects the two minima[21,22]. Although quite powerful if the landscape is not too rough, the method has the drawback that one needs to know that the two minima considered are really neighbors, i.e. that the two basins of attraction touch each other. This problem is also present for more involved algorithms, such as the transition path sampling method[23].

2. The second class of methods needs instead only one starting minimum and uses the information on the local geometry of the PEL to climb up the landscape until a saddle point is found. Popular realizations of this approach are the dimer method[24,25], the eigenvector-following method[7,26] and the Lanczos algorithm of the "ART nouveau" method[27],

all of which are based on the idea to determine and then follow the direction of the smallest curvature of the PEL, i.e. the softest mode of the Hessian matrix. With such a "slowest ascent" protocol the search is guaranteed to converge to a transition state of the PEL. Although these methods are suited for, e.g., the analysis of small clusters of Lennard-Jones particles[5,8], not all of them are applicable to large systems since most of them require at each iteration step the evaluation and inversion of the Hessian matrix, a numerical effort that scales like $\mathcal{O}(N^3)$. A notable exception is the so-called "dimer-method" which does not require information on the second derivatives[24]. Another drawback of these approaches is that they do not guarantee to find the lowest saddle point but instead one that is determined on how the algorithm is started[28]. In practice it thus can happen that the saddle points that are found are very high up in the PEL and therefore physically irrelevant[29]. Furthermore, it is sometimes also problematic to escape the local well of the PEL near to the IS in a non-trivial direction, since the softest eigenmode actually corresponds to the translational and rotational zero-frequency modes[30].

Other methods have been proposed to find a reaction path that gives the escape route from a local minimum[31]. Although these methods are very efficient if the system is not too complex, they are not adapted to the case where one has many degrees of freedom.

3. Finally we mention an approach to locate saddle points that does not make use at all of the minima of the PEL and that has been employed with some success in the field of supercooled liquids and glasses, see, e.g.,[12,15,16]. For this one considers the squared gradient of the potential energy $W = |\vec{\nabla} V|^2$. The idea is that since at a saddle point one has $\vec{\nabla} V = 0$, a minimization of W will lead to a saddle point or a local minimum. However, in practice one finds that this approach has the drawback that i) there are many stationary points in the PEL that are neither saddle points nor minima and ii) that there are also many "quasi-saddles", i.e. a local shoulder in the PEL at which the derivative is not zero but has only a local minimum (i.e. an inflection point) and which thus shows up in W as a local minimum[29,32,33]. Since at low temperatures, i.e. when one is deep down in the PEL, the number of these quasi-saddles starts to become much larger than the number of true minima or SPs this approach becomes very inefficient.

In this paper we propose a new method that allows to locate low lying saddle points associated with a given local minimum. The algorithm makes only use of the value of the potential energy as well as its gradient, i.e. there is no need to calculate the numerically expensive Hessian matrix used by some other algorithms. The rest of the paper is structured as follows: In the following section we introduce the new class of algorithms. In Sec. III we give the details on the two systems that we will use to test the efficiency of the algorithms and in Sec. IV we give the results of these tests. Finally we summarize and conclude in Sec. V.

II. ALGORITHM TO FIND THE SADDLE POINT

The idea of the algorithm, which we name "discrete difference slowest ascent" (DDSA), is to locate the saddle points of $V(\{\mathbf{r}_i\})$ with the help of a new cost function $H_{\mathrm{DDSA}}(\mathbf{X}, \beta)$ which can be minimized without using the computationally expensive Hessian matrix. Here $\mathbf{X}$ represents the coordinates of all the particles and β is a parameter the meaning of which will be discussed below. Since our algorithm has a certain similarity to the one proposed by Duncan *et al.*, Ref. [34], we briefly discuss the latter and point out the differences.

In the "Biased Gradient Square Descent" (BGSD) algorithm of Ref. [34] for finding transition states one starts at a local minimum of $V(\mathbf{X})$ that in the following we will refer to as $\mathbf{X}_{\mathrm{IS}}$, where "IS" stands for "inherent structure". The BGSD algorithm is based on the idea of introducing an auxiliary cost function the minimization of which allows to climb up the PEL in the direction of the SP of $V(\mathbf{X})$ that is close to $\mathbf{X}_{\mathrm{IS}}$. The proposed cost function is given by

$$H_{\mathrm{BGSD}}(\mathbf{X}; \alpha, \beta) = \frac{1}{2}|\nabla V(\mathbf{X})|^2 + \frac{1}{2}\alpha(V(\mathbf{X}) - \beta)^2 \quad . \quad (1)$$

So the first term is identical to the potential W discussed in the introduction. The second term makes that the minimization algorithm will seek to minimize this squared gradient with the constraint that the potential energy has a value β. Thus if one sets the energy β to a value that is slightly higher than the local minimum, the algorithm will make a compromise between the smallest absolute value of the gradient and an energy that is as close as possible to β. The balance between these two terms is given by the prefactor α. Once the local minimum has been found, the value of β is increased a bit, thus allowing iteratively to climb up the PEL until a saddle point is found.

The drawback of this approach is that usually the algorithm for the minimization of $H_{\mathrm{BGSD}}(\mathbf{X}; \alpha, \beta)$ will need the first derivative of the cost function, i.e. in the case of Eq. (1) the second derivative of $V(\mathbf{X})$, a calculation that becomes very expensive if the number of particles is large. Therefore Duncan *et al.* have proposed to make use of the relation
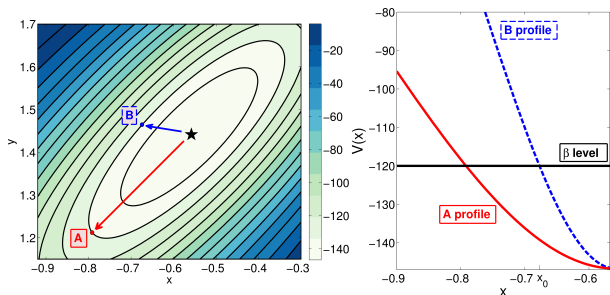
FIG. 1. Left: Schematic plot showing possible paths to climb up the PEL that has a local minimum (star). The points A and B lie on the same iso-potential line of height β, but the slope at A is less than that one at B. As a consequence the DDSA algorithm will choose the point A. Right: Representation of the one-dimensional profile of the potential surface: The solid line indicates the profile in the direction of point A while the dashed line in the direction B. The horizontal line indicates the energy level β used in the DDSA algorithm.

$$\nabla^2 V(\mathbf{X})\nabla V(\mathbf{X}) = \lim_{\delta \to 0} \frac{\nabla V[\mathbf{X} + \delta\nabla V(\mathbf{X})] - \nabla V(\mathbf{X})}{\delta} \tag{2}$$

and to approximate the right hand side by a finite difference quotient using a small value of δ. Although this approximation is reasonable if the number of degrees of freedom is not too large, it usually becomes inaccurate for N large (if δ is kept fixed). The algorithm that we present in the following avoids this problem since it does not need the second derivative of $V(\mathbf{X})$ and hence no approximation of the type given by Eq. (2) is necessary.

The idea of our DDSA algorithm is to introduce a new cost function $H_{\mathrm{DDSA}}(\mathbf{X}, \beta)$ that has the same local extrema as $V(\mathbf{X})$ but which does not involve the gradient of $V(\mathbf{X})$ and hence H_{DDSA} can be optimized without the need of calculating the Hessian matrix. Furthermore this function should allow to identify the direction of the PEL that has the smallest slope and hence admit to ascend the PEL in the softest direction. The cost function we propose is given by

$$H_{\mathrm{DDSA}}(\mathbf{X}, \beta) = [V(\mathbf{X}) - \beta]^2 + [V(\mathbf{X} + \Delta\mathbf{X}) - \beta]^2 \tag{3}$$

where $\Delta\mathbf{X}$ is a small displacement in phase space (details are given below) and β is a target energy value.

To understand the idea of this algorithm it is useful to start with a simple two-dimensional example, a cartoon of which is show in Fig. 1. In panel a) we show the iso-potential lines of the PEL around a local minimum, represented by a star. Consider two lines that start at this minimum. Line "A" is in the direction of the softest mode, i.e. slowest ascent, while direction "B" has a steeper slope. In panel b) we show a cut of the PEL in the direction of A and B. Let us consider these one-dimensional cuts of the potential in the neighborhood of $x = x_0$, where x_0 is defined via $V(x_0) = \beta$ and β is
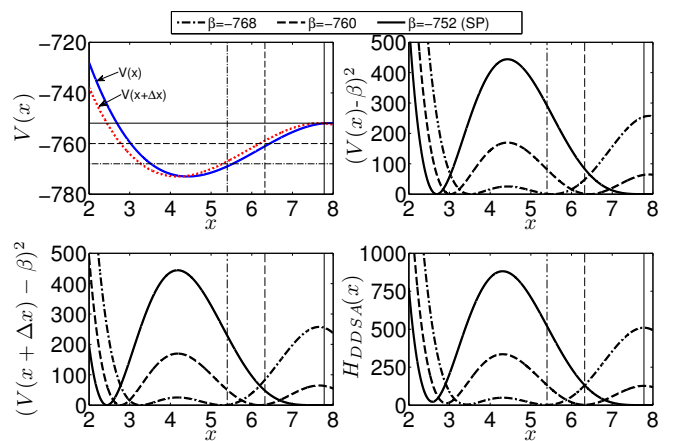

FIG. 2. Contributions of the various terms in the cost-function H_{DDSA} for a one-dimensional case. a) Original potential $V(x)$ (full line) and $V(x + \Delta x)$ for $\Delta x = 0.25$ (dotted line). The horizontal lines correspond to different energy values β. The vertical lines show the location of the minimum of H_{DDSA} for the different values of β. b) The first term on the right hand side of Eq. (3) for the three values of β of panel a). c) The second term on the right hand side of Eq. (3) for the three values of β of panel a). d) The final cost function H_{DDSA} for the three values of β of panel a).

a given value of the potential energy. Making a Taylor expansion of $V(x)$ around x_0 gives for $H_{\mathrm{DDSA}}(x, \beta)$

$$H_{\mathrm{DDSA}}(x_0 + \epsilon, \beta) \approx [2\epsilon^2 + 2\epsilon\Delta x + (\Delta x)^2][V'(x_0)]^2 \quad . \tag{4}$$

One sees easily that the minimum of this function is given if ϵ is chosen to be $-\Delta x/2$. From Eq. (4) one finds that the value of H_{DDSA} at this minimum is given by $[\Delta V'(x_0)]^2/2$, i.e. it is proportional to $[V'(x_0)]^2$. Thus we can conclude that the minimum of the function H_{DDSA} is given by a point at which the gradient is as small as possible since this is the best compromise between the first and second term on the right hand size of Eq. (3). The influence of the various terms and steps of this procedure are shown in Fig. 2.

It is easy to see that this argument can be generalized to the case with many degrees of freedom if one replaces the quantity ϵ in Eq. (4) by $\epsilon\nabla V(\mathbf{X}_0)$, where $\mathbf{X}_0$ is a point with $V(\mathbf{X}_0) = \beta$. This implies that the minimization of the function H_{DDSA} from Eq. (3) will give a point that is close to the energy level β and that has the smallest gradient.

We now return to the displacement $\Delta\mathbf{X}$ given in Eq. (3). This displacement has to fulfill two requirements: i) it should be small so that the Taylor expansion used above is valid and ii) the point $\mathbf{X} + \Delta\mathbf{X}$ should *not* be on the energy surface of value β since in that case both terms in Eq. (3) can be made to vanish. It is of course easy to fulfil the first condition. The second one can be taken care of by choosing the direction of $\Delta\mathbf{X}$ as
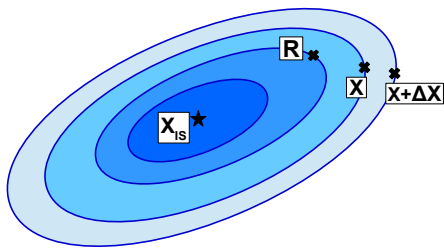
FIG. 3. Illustration of the points used in the DDSA algorithm for the case of a two-dimensional energy landscape. $\mathbf{X}_{\text{IS}}$ is the local minimum of the landscape, $\mathbf{R}$ is the reference point used in the search, and $\mathbf{X}$ and $\mathbf{X} + \Delta\mathbf{X}$ are the points used to find the path of the slowest ascent.

$$\widehat{\Delta\mathbf{X}} = \frac{\mathbf{X} - \mathbf{R}}{|\mathbf{X} - \mathbf{R}|} \quad , \qquad (5)$$

where the position $\mathbf{R}$, called in the following "reference point", will be discussed in Sec. IV. But already here we can state that $\mathbf{R}$ will be chosen such that $V(\mathbf{R}) < \beta$, i.e. the vector $\widehat{\Delta\mathbf{X}}$ from Eq. (5) is not parallel to an iso-line and points upward in the PEL (see Fig. 3 for an illustration).

The cost function H_{DDSA} defined by Eq. (3) and the displacement vector $\Delta\mathbf{X}$ from Eq. (5) allows to find the path of slowest ascent. (In Sec. IV we will discuss how the magnitude of $\Delta\mathbf{X}$ has to be chosen.) We have found that in practice the efficiency of the algorithm depends also on how the starting point for the iteration is chosen[35]. In the following we will denote this starting point by $\mathbf{G}$ and explain in Sec. IV how we have chosen it.

III. SYSTEMS

In this section we describe the two systems which we have used to test the performance of the DDSA algorithm. Although both of them have only two degrees of freedom, they have already many of the complexities encountered in higher dimensional PELs and therefore they can be considered as instructive test cases for the algorithm.

The first system is the well known Müller-Brown (MB) potential, a model which was introduced to describe a simple PEL and whose properties have been studied extensively, notably to test the performance of various algorithms aimed to find a reaction path[5,29,36–38].

The MB potential is the sum of four Gaussians and is given by

$$V_{\text{MB}}(x,y) = \sum_{i=1}^{4} A_i \exp[a_i(x - \bar{x}_i)^2 + \qquad (6)$$
$$b_i(x - \bar{x}_i)(y - \bar{y}_i) + c_i(y - \bar{y}_i)^2] \quad (7)$$

where

$$A = (-200, -100, -170, 15); \quad a = (-1, -1, -6.5, 0.7)$$
$$b = (0, 0, 11, 0.6); \quad c = (-10, -10, -6.5, 0.7)$$
$$\bar{x} = (1, 0, -0.5, -1); \quad \bar{y} = (0, 0.5, 1.5, 1).$$
$$(8)$$

A contour plot for this potential is shown in Fig. 4a and we recognize the presence of two minima, marked by "IS", separated by a saddle point (SP). The graph shows that a slowest ascent path is not very curved, thus it should not be that difficult for an algorithm to find it. Since, however, in practice one must expect that the PEL has a slowest ascent path that is more windy, we have also considered a PEL that is from this point of view a bit more challenging. This modified Müller-Brown (MMB) surface is given by the MB potential to which we have added a further term:

$$V_{\text{MMB}}(x,y) = V_{\text{MB}}(x,y) + V_{\text{add}}(x,y) \quad . \qquad (9)$$

This additional term is given by

$$V_{\text{add}}(x,y) = A_5 \sin(xy) \exp[a_5(x - \bar{x}_5)^2 + c_5(y - \bar{y}_5)^2] \qquad (10)$$

with

$$\bar{x}_5 = -0.5582; \quad \bar{y}_5 = 1.4417$$
$$A_5 = 500; \quad a_5 = -0.1; \quad c_5 = -0.1 \qquad (11)$$

This additional term makes that now the valley emanating from the main minimum is bending away from the original saddle point (now at the lower right corner of Fig. 4b), making it thus more difficult for an algorithm to find this point. In addition the second term has also created a second saddle point in the PEL (upper left corner in Fig.4b) that has a higher barrier than the original saddle point of the MB surface. Thus we are seeking an algorithm that is able to find the lower saddle point and not the higher one.

IV. TEST OF THE ALGORITHM

In this section we will introduce four versions of the DDSA algorithm and discuss how they fare in finding the saddle points in the PELs defined by the MB and MMB potentials. All algorithms have the same basic structure: i) Given a starting point $\mathbf{Y}$, we choose a new target energy $\beta = V(\mathbf{Y}) + \delta$ (with $\delta > 0$), a reference point $\mathbf{R}$, as well as a starting point for the search, $\mathbf{G}$; ii) We minimize the cost function $H_{\text{DDSA}}(\mathbf{X}, \beta)$ and find a new point on the slowest ascent path that has an energy close to β. Then we restart the iteration. In the following we will denote by "level n" the n'th iteration
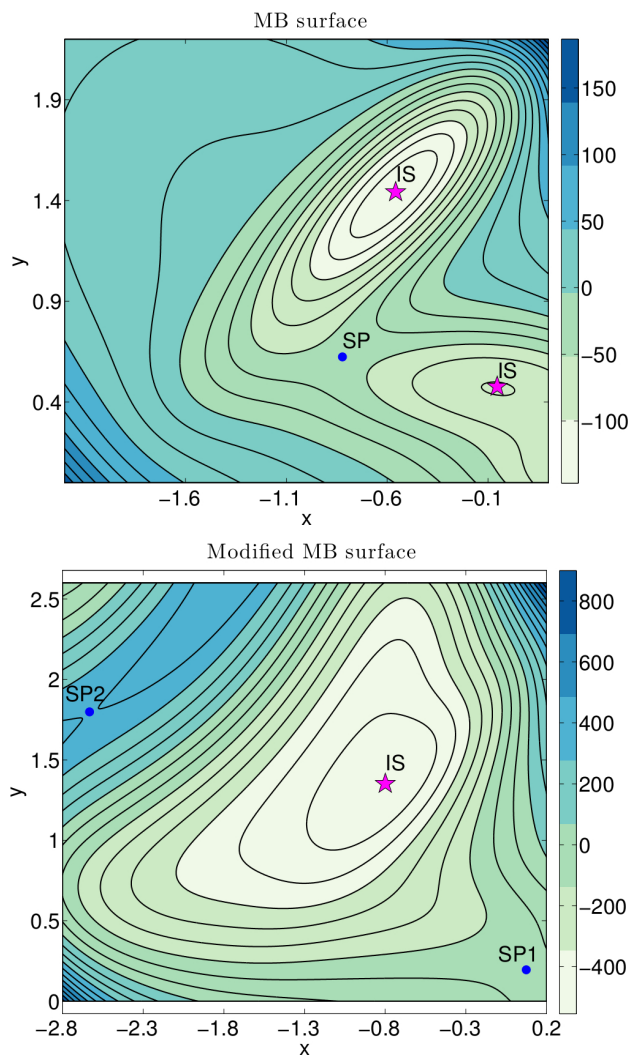
FIG. 4. Contour plots of the Müller-Brown potential, panel a), and modified Müller-Brown potential, panel b). The local minima are shown as red stars (IS) and the saddle points as blue circles (SP).
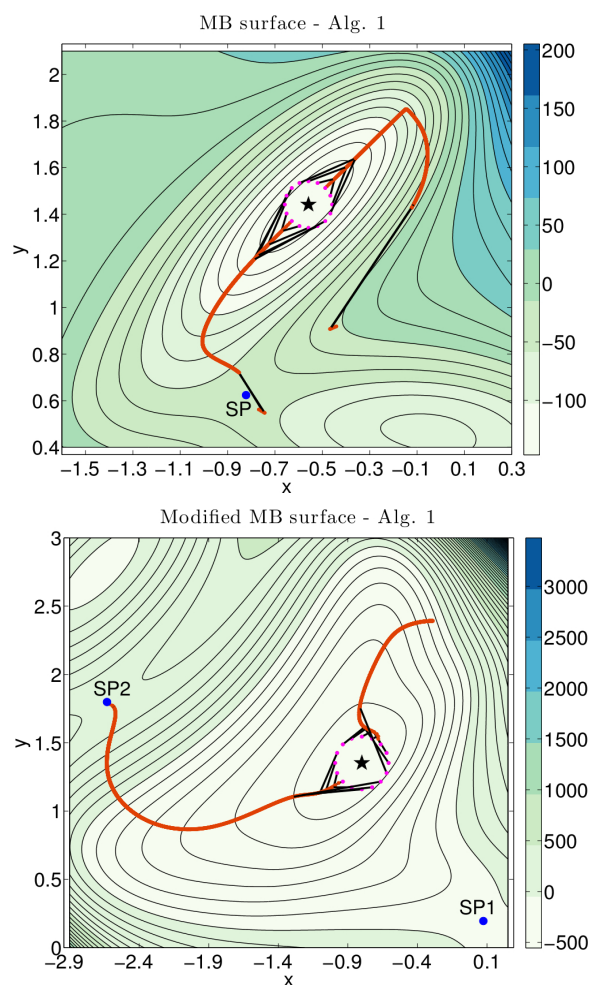

FIG. 5. Algorithm 1: Trajectories that start from the pink points around the local minimum of the PEL (star). a) Müller-Brown surface, b) modified Müller-Brown surface. Note that for the MMB surface some of the trajectories lead up to the SP2 which is higher than SP1.

of this procedure. The main difference between the versions of the algorithm is the choice of the reference point $\mathbf{R}$ and of the point $\mathbf{G}$.

Algorithm 1: The first form of the DDSA algorithm uses the following expressions for $\mathbf{R}$, $\Delta\mathbf{X}$, and $\mathbf{G}$:

$$\mathbf{R} = \mathbf{X}_{\text{IS}} \qquad (12)$$

$$\Delta\mathbf{X} = \frac{\epsilon(\mathbf{X} - \mathbf{R})}{|\mathbf{X} - \mathbf{R}|} \qquad (13)$$

$$\mathbf{G} = \mathbf{X}_{\text{min}(n-1)} - \frac{\delta}{|\nabla V(\mathbf{X}_{\text{min}(n-1)})|} \cdot \frac{\nabla V(\mathbf{X}_{\text{min}(n-1)})}{|\nabla V(\mathbf{X}_{\text{min}(n-1)})|} \qquad (14)$$

Here $X_{\text{min}(n)}$ is the minimum obtained from the iteration number n. With this choice of $\mathbf{R}$ the vector $\Delta\mathbf{X}$ points thus in the direction of the local minimum at which we start the slowest ascent. The quantity ϵ is the magnitude of this displacement and we choose $\epsilon = 0.001$ and 0.01 for the MB and MMB potential, respectively. For δ we have chosen 0.5 (MB) and 4.1 (MMB). These values are appropriate for the length scales occurring in the MB or MMB PEL (see Fig. 4), but they do not need to be fine-tuned. From Eq. (14) we see that the position $\mathbf{G}$ at which we start the iteration is given by the position of the previous minimum plus a vector that points in the opposite direction of the gradient of the PEL and that has a length which is just a linear extrapolation of this gradient to the energy level β.

To test the efficiency of this algorithm we have used 16 starting points arranged on a circle of radius r_0 around the minimum $\mathbf{X}_{\text{IS}}$, using a radius r_0 of 0.1 and 0.2 for the

MB and MMB potential, respectively. This setup allows thus to estimate the probability that the algorithm finds the lowest saddle point. Defining one of these starting points as $\mathbf{X}_{\min(1)}$, we choose as target energy $V(\mathbf{X}_{\mathrm{IS}}) + \delta$ and use Eq. (14) to obtain the starting point $\mathbf{G}$ for the optimization of the cost function H_{DDSA} of Eq. (3). This optimization was done by means of the Polak-Ribiere variant of the conjugate gradient algorithm[10]. Note that the quantities $\mathbf{R}$ and $\mathbf{G}$ are fixed during the search of the minimum of $H_{\mathrm{DDSA}}(\mathbf{X}, \beta)$, i.e. the calculation of the gradient of this cost function for the optimization does not involve the calculation of a second derivative of $V(\mathbf{X})$.

In Fig. 5a we show the trajectories obtained from the 16 starting points in the MB potential. We see that all trajectories that start toward the lower left direction converge rapidly onto a master curve that does indeed correspond to the path of slowest ascent. For the starting points that lie on the upper right half of the circle the resulting trajectories first follow the slowest ascent path in that direction, i.e. a direction that does not really lead to the correct saddle point. However, at a certain point in the ascent the gradient becomes so large that the algorithm finds a direction in which the gradient is smaller that the simple upward direction and thus the trajectory starts to turn. Although in this case the algorithm does not pass at the saddle point (since it has climbed up too far), it is able to come quite close to the sought saddle point. In that case a steepest descent procedure using the cost function $W = |\nabla V|^2$ and the approximation of Eq. (2) would allow to locate the saddle point with good precision. Thus by monitoring the value of W it would be easy to realize that the algorithm has entered in a sector of configuration space in which one of the eigenvalues of the Hessian matrix has become negative, i.e. that one has entered a new basin of attraction for the potential W and the minimum of this basin is most likely the one of the saddle point.

For the case of the MMB potential the algorithm performs not so well, Fig. 5b. We see that the trajectories that start on the lower left part of the circle all end up at the saddle point SP2, i.e. the algorithm manages to find a saddle point, but it is not the lowest one. The reason for this failure in the case of the MMB surface is related to the fact that the reference point $\mathbf{R}$ is fixed at $\mathbf{X}_{\mathrm{IS}}$ and thus the vector $\Delta \mathbf{X}$, used to define the point at which the second term of $H_{\mathrm{DDSA}}(\mathbf{X}, \beta)$ is evaluated, does not adapt to the shape of the local PEL close to $\mathbf{X}$ since $\Delta \mathbf{X}$ always points to the local minimum $\mathbf{X}_{\mathrm{IS}}$. This is no problem as long at the ascending valley is not curved and emanates in a more or less straight manner from $\mathbf{X}_{\mathrm{IS}}$. However, if there is a noticeable curvature, as it is the case for the MMB PEL, the iso-potential lines are no longer (almost) orthogonal to the vector $\Delta \mathbf{X}$ which makes that the minimum of the cost function $H_{\mathrm{DDSA}}(\mathbf{X}, \beta)$ is no longer the slowest ascent. It can thus be expected that a reference point $\mathbf{R}$ that adapts to the local shape of the PEL will help to alleviate this problem. This is the idea of the next version of the algorithm.

Algorithm 2: This version of the DDSA algorithm uses a reference point that is moving along with the slowest ascent trajectory. The simplest way to do this is to pick on level n of the path for $\mathbf{R}$ the location of the minimum found on the previous level, i.e. $\mathbf{X}_{\min(n-1)}$. However, we have found that this choice leads to numerical instabilities and thus the ascent trajectory becomes very erratic[35]. In algorithm 2 we try to avoid this problem by choosing as reference point the minimum that has been found k levels earlier, where k is an integer. In addition we have also adapted the magnitude of the displacement $\Delta \mathbf{X}$ to take into account the steepness of the PEL in the vicinity of $\mathbf{X}$. Thus the algorithm is given by

$$\mathbf{R} = \begin{cases} \mathbf{X}_{\mathrm{IS}} & \text{if } n \leq k \\ \mathbf{X}_{\min(n-k)} & \text{if } n > k \end{cases} \tag{15}$$

$$\Delta \mathbf{X} = \frac{\delta}{|\nabla V(\mathbf{X}_{\min(n-k)})|} \cdot \frac{\mathbf{X} - \mathbf{R}}{|\mathbf{X} - \mathbf{R}|} \tag{16}$$

$$\mathbf{G} = \mathbf{X}_{\min(n-1)} \quad . \tag{17}$$

Thus for the first k steps of climbing up the PEL we keep the IS as the reference point, i.e. we assume that the PEL has a simple geometry without winding valleys. After having reached level $k + 1$ one uses for $\mathbf{R}$ the minimum $\mathbf{X}_{\min(1)}$, subsequently $\mathbf{X}_{\min(2)}$ and so on. In this algorithm we chose the magnitude of the displacement vector $\Delta \mathbf{X}$ such that it adapts to the local slope (see the first factor on the RHS of Eq. (16)). The values for δ were 0.50 and 0.25 for the MB and MMB potential, respectively. Note that for this version of the algorithm we have also modified the starting point $\mathbf{G}$ for the minimization of $H_{\mathrm{DDSA}}(\mathbf{X}, \beta)$ since we have found that for the performance of the algorithm it doesn't really matter whether we chose the point given by the RHS of Eq. (14) or the simpler expression given by Eq. (17)[35]. The values of k were chosen to be 25 and 100 for the MB and MMB potential, respectively. These numbers and the values of δ imply that the reference point $\mathbf{R}$ is about 12.5 (MB) and 25 (MMB) energy units below the energy at which one seeks the local minimum of the slope. This energy value corresponds thus roughly to the scale on which the shape of the PEL is significantly deformed.

In Fig. 6 we show the trajectories obtained from this algorithm. For the case of the MB surface we find that this algorithm has a much better performance than algorithm 1 in that even the points that start on the upper right half of the circle around $\mathbf{X}_{\mathrm{IS}}$ converge to the SP. For intermediate times we find that these latter trajectories show a bit of jittering when they jump to the lower left valley, but this motion is quickly damped out.

However, for the case of the MMB surface, also this algorithm is not able to find the saddle point, see Fig. 6b.
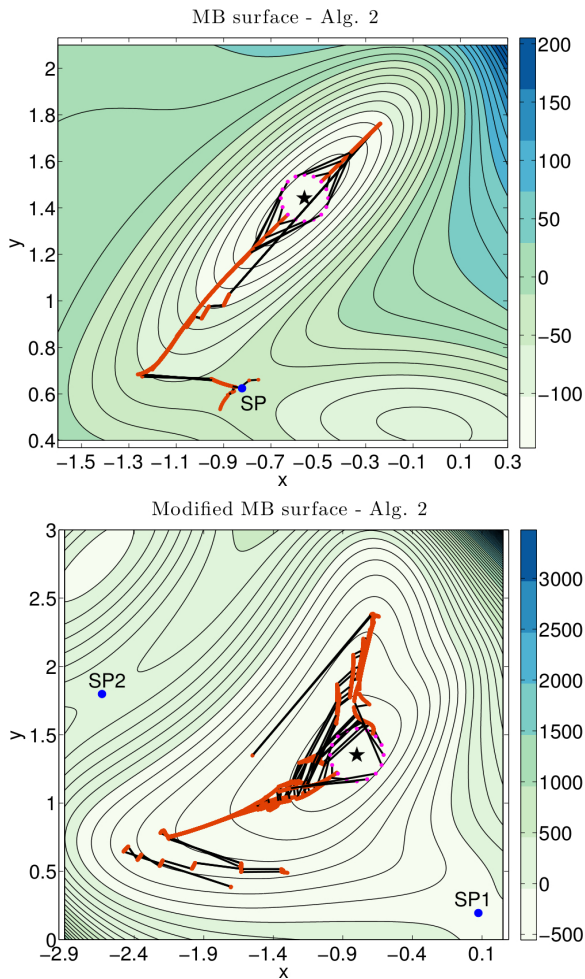
FIG. 6. Algorithm 2: Trajectories that start from the pink points around the local minimum of the PEL (star). a) Müller-Brown surface, b) modified Müller-Brown surface. Note that for both PELs there are certain trajectories that are somewhat erratic.
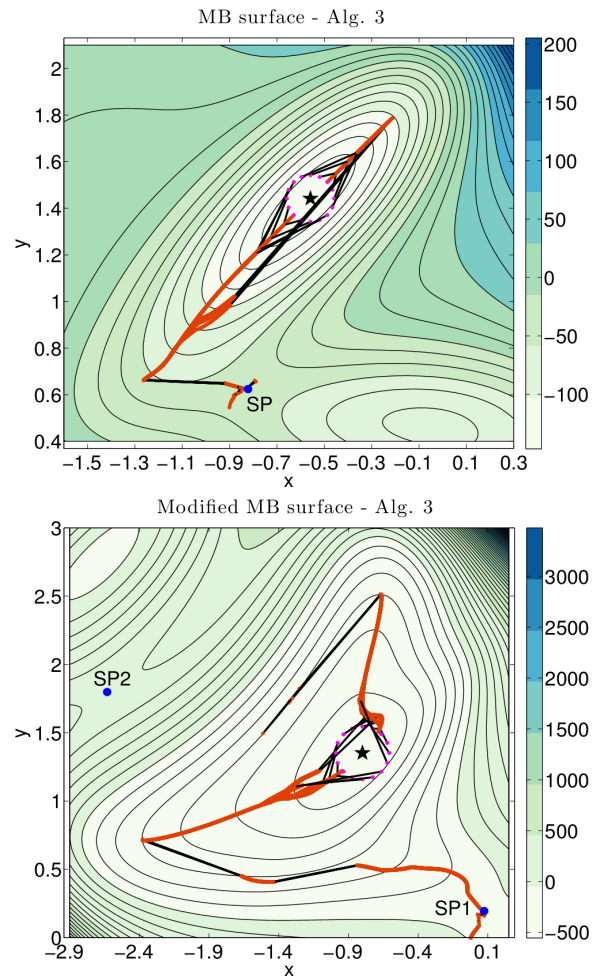
FIG. 7. Algorithm 3: Trajectories that start from the pink points around the local minimum of the PEL (star). a) Müller-Brown surface, b) modified Müller-Brown surface. Note that for the MMB PEL some of the trajectories arrive at the lowest lying saddle point SP1.

The reason for this is that at a certain energy level the trajectory becomes very erratic which in turn has the effect that also the reference point $\mathbf{R}$ moves around in an uncontrolled manner. As a consequence the algorithm fails to climb up further. Thus this behavior is qualitatively the same as the one we described at the beginning of the section on algorithm 2, i.e. the case that corresponds to $k = 1$. This undesirable behavior is related to a nonlinear feedback mechanism between the choice of the reference point for the optimization on level n and the minimization procedure: On one level $\mathbf{R}$ is slightly on one side of the slowest ascent valley, and on the next level $\mathbf{R}$ jumps on the other side of the valley and has increased somewhat the distance to it, leading to the observed zig-zag motion[35].

To cope with this problem we have introduced a further version of the DDSA algorithm:

Algorithm 3: One possibility to avoid the instability

that we have encountered with algorithm 2 is to use the information on the ascent trajectory to define the reference point $\mathbf{R}$ and to damp out the small fluctuations in its location that lead to the numerical instabilities discussed above. In practice we do this by defining $\mathbf{R}$ as the average over a certain number k of previous positions $\mathbf{X}_{\min}$. Thus at level n the algorithm is given by

$$\mathbf{R} = \begin{cases} \mathbf{X}_{\text{IS}} & \text{if } n \leq k \\ \frac{1}{k} \sum_{i=n-k}^{n-1} \mathbf{X}_{\min(i)} & \text{if } n > k \end{cases} \quad (18)$$

$$\Delta \mathbf{X} = \frac{\delta}{|\nabla V(\mathbf{X}_{\min(n-k)})|} \cdot \frac{\mathbf{X} - \mathbf{R}}{|\mathbf{X} - \mathbf{R}|} \quad (19)$$

$$\mathbf{G} = \mathbf{X}_{\min(n-1)} \quad . \quad (20)$$

For k we have chosen 50 (MB) and 165 (MMB) and $\delta = 0.5$ (MB and MMB). That this version is indeed able to find the SPs for both the MB and MMB potentials is shown in Fig. 7. For the case of the MB PEL all 16 trajectories lead up to the lowest lying SP. In contrast to the results for algorithm 2, all the trajectories are now very smooth thus indicating that the damping mechanism is indeed able to suppress the numerical instability of the previous version.

For the MMB surface we find that 10 out of 16 trajectories reach the *correct* saddle point, Fig. 7b, thus showing that this algorithm is indeed much more performant than the two previous ones. Also for this PEL the ascending trajectories have become much smoother, indicating that the numerical instability is no longer present.

The way the DDSA algorithm is set up, it will attempt to follow the path of the slowest ascent, an approach that it shares with other algorithms, such as, e.g. the dimer method[24]. However, as discussed above, this path does not necessarily lead to the lowest saddle point since the latter might (locally) involve a steeper path. It is therefore useful to probe not only the slowest ascent path, but also trajectories that are from time to time a bit steeper. This is the underlying idea of the next algorithm.

Algorithm 4: This algorithm introduces noise in the generation of the ascending trajectory and it is given by the following choice of the parameters:

$$\mathbf{R} = \begin{cases} \mathbf{X}_{\text{IS}} & \text{if } n \leq k \\ \frac{1}{k}\sum_{i=n-k}^{n-1} \mathbf{X}_{\text{min(i)}} & \text{if } n > k \end{cases} \quad (21)$$

$$\Delta\mathbf{X} = \frac{\epsilon(\mathbf{X} - \mathbf{R})}{|\mathbf{X} - \mathbf{R}|} \quad (22)$$

$$\mathbf{G} = \mathbf{X}_{\text{min}(n-1)} + \mathbf{Z} \quad \text{with } \mathbf{Z} \cdot \nabla V(\mathbf{X}_{\text{min}(n-1)}) = 0 \quad . \quad (23)$$

Thus the algorithm includes a reference position $\mathbf{R}$ the motion of which is damped by averaging over several local minima. (We have used $k = 30$ and 250 for the MB and MMB PELs, respectively.) The displacement vector $\Delta\mathbf{X}$ is the simple expression already used in algorithm 1 with $\epsilon = 10^{-2}$ and 10^{-4} for the MB and MMB potentials, respectively. The main novelty of this algorithm with respect to the previous ones is the presence of a random vector $\mathbf{Z}$ in the definition of the point $\mathbf{G}$ that is used to start the iteration. This random vector $\mathbf{Z}$ is orthogonal to $\nabla V(\mathbf{X}_{\text{min}(n-1)})$ and has magnitude γ, where γ is a uniformly distributed random number in the interval $[0, \gamma_0]$. The maximum value we chose for the magnitude of $\mathbf{Z}$ was $\gamma_0 = 10^{-3}$ (MB) and 0.0052 (MMB). The presence of this random vector in the definition of the initial position $\mathbf{G}$ gives the algorithm a chance to depart to some extent from the slowest ascent trajectory. That this flexibility can indeed be needed for finding the lowest lying
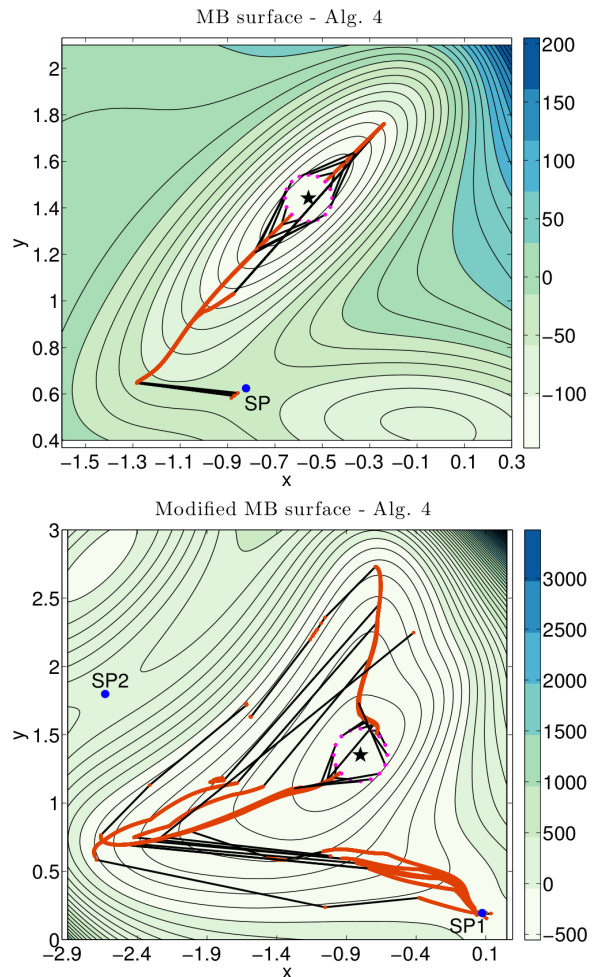

FIG. 8. Algorithm 4: Trajectories that start from the pink points around the local minimum of the PEL (star). a) Müller-Brown surface, b) modified Müller-Brown surface. Note that for the MMB PEL most of the trajectories arrive at the lowest lying saddle point SP1.

SP can be recognized from the MMB PEL: In Fig. 5b the steepest ascent path leads up to the higher SP and thus is missing the path that goes to the lower SP because the latter path is locally, i.e. where the two paths meet, a bit steeper than the former one. Therefore an algorithm that follows only the slowest ascent will not be able to find SP1.

The trajectories obtained from this version of the DDSA algorithm are shown in Fig. 8. We see that for the case of the MB potential all 16 trajectories lead up to the SP, Fig. 8a. For the case of the MMB potential 13 out of 16 trajectories reach the lowest lying SP, 8b, thus showing that algorithm 4 has a better performance than the ones we have presented previously. Hence we can conclude that the presence of weak noise in the search improves the efficiency of the algorithm.

Version	MB	MMB
	Success in finding SP	Success in finding SP
1	8/16	0/16
2	16/16	0/16
3	16/16	10/16
4	16/16	13/16

TABLE I. Comparing the success rate of the different versions of the DDSA algorithm applied to the MB and MMB surface.

V. CONCLUSION

We have introduced a new class of algorithm that allows to find low lying saddle points in complex potential energy landscapes. The algorithm makes only use of the potential and its first derivative, thus quantities that are usually readily available and hence do not need extra coding/calculations. In particular the algorithm does not need any information about the second derivatives of the potential energy and hence scales very favorably with the number of degrees of freedom, this in contrast to other algorithms that need information about the Hessian matrix. The basic idea of the algorithm is to evaluate the potential at two different points and to use this information to locate the direction that has the slowest ascent. This class of algorithm, that we denote as "Discrete Difference Slowest Ascent" has a few parameters the choice of which influences the performance of the algorithm. Using the Müller-Brown potential as well as a modification of this potential as test cases we have looked into four possible choices of these parameters and identified two as the relevant ones: 1) the reference point that is used to determine the relative position of the two points mentioned above and 2) the starting point for the local optimization. A summary of the result of our tests is presented in Table I. We recognize that the MB PEL is a relatively easy case for the algorithm in that it finds the correct SP as soon as the reference point $\mathbf{R}$ is allowed to move. More difficult is the case of the MMB PEL in which the lowest SP is not directly connected to the slowest ascent path. Algorithm 2 fails to find this lowest SP, but is able to find the SP that is directly connected to the slowest ascent path. This case is thus an example that illustrates that algorithms which follow just the eigenvector with the smallest eigenvalue do not necessarily lead to the *lowest* SP. This problem is partially overcome by algorithm 3 since the reference point $\mathbf{R}$ can (sometimes) help to change the trajectory in the direction of the lowest SP. To overcome this problem in a more systematic manner it is, however, necessary to allow the algorithm to follow at least locally a "non-optimal" path, i.e. to deviate from the slowest ascent valley, since this will allow it to discover additional valleys that (potentially) lead to low lying saddle points. Our algorithm 4 does permit such locally non-optimal trajectories and fares indeed significantly better to find the correct SP.

Although we have considered here only PELs that depend on two degrees of freedom, there is no reason to expect that the DDSA algorithm will not do well also in cases in which the cost function depends on many degrees of freedom. In such complex systems it still can be expected that the total number of valleys that emanate from a local minimum is a linear function of the number of particles. Hence this will not really add an increased numerical complexity. Since the DDSA algorithm allows to follow each of these valleys in a numerical effort that is linear in the number of degrees of freedom, and the introduced randomness will not change this, it should be possible to locate the saddle points in an efficient manner. Hence we conclude that the DDSA algorithm presented here is a promising approach to probe the properties of complex PELs. The presence of a weakly random component allows it to locate low-lying saddle points even in cases in which certain completely deterministic algorithms will fail. Hence the algorithm should be able to find solutions to optimization problems, such as reaction paths, that so far have been outside of reach of a reasonable numerical effort.

[1] D.J. Wales, *Energy Landscapes: Applications to Clusters, Biomolecules and Glasses* (Cambridge University Press, 2003).

[2] M. Goldstein, "Viscous liquids and the glass transition: A potential energy barrier picture," The Journal of Chemical Physics **51**, 37283739 (1969).

[3] G. Jug, S. Bonfanti, and W. Kob, "Realistic tunnelling states for the magnetic effects in non-metallic real glasses," Philosophical Magazine **96**, 648 (2016).

[4] F.H Stillinger, "Exponential multiplicity of inherent structures," Physical Review E **59**, 48 (1999).

[5] D. J. Wales, "Rearrangements of 55-atom Lennard-Jones and $(C_{60})_{55}$ clusters," The Journal of Chemical Physics **101**, 3750 (1994).

[6] D.J. Wales, M.A. Miller, and T.R. Walsh, "Archetypal energy landscapes," Nature **394**, 758 (1998).

[7] D.J. Wales and J.P.K. Doye, "Stationary points and dynamics in high-dimensional systems," The Journal of Chemical Physics **119**, 12409 (2003).

[8] J.P.K. Doye, M.A. Miller, and D.J. Wales, "Evolution of the potential energy surface with size for Lennard-Jones clusters," The Journal of Chemical Physics **111**, 8417 (1999).

[9] D.J. Wales, "Insight into reaction coordinates and dynamics from the potential energy landscape," The Journal of Chemical Physics **142** (2015).

[10] W. Press, S. Teukolsky, W. Vetterling, and B. Flannery, *Numerical Recipes in Fortran 77: The Art of Scientific Computing* (Cambridge University Press, New York, 1992).

[11] T. A. Weber and F. H. Stillinger, "Inherent structures and distribution functions for liquids that freeze into bcc crystals," The Journal of Chemical Physics **81**, 5089 (1984).

[12] T.A. Weber and F.H. Stillinger, "Interactions, local order, and atomic-rearrangement kinetics in amorphous nickel-phosphorous alloys," Physical Review B **32**, 5402 (1985).

[13] A. Heuer, "Properties of a glass-forming system as derived from its potential energy landscape," Physical Review Letters **78**, 4051 (1997).

[14] S. Sastry, P. G. Debenedetti, and F. H. Stillinger, "Signatures of distinct dynamical regimes in the energy landscape of a glass-forming liquid," Nature **393**, 554 (1998).

[15] L. Angelani, R. Di Leonardo, G. Ruocco, A. Scala, and F. Sciortino, "Saddles in the energy landscape probed by supercooled liquids," Physical Review Letters **85**, 5356 (2000).

[16] K. Broderix, K.K. Bhattacharya, A. Cavagna, A. Zippelius, and I. Giardina, "Energy landscape of a Lennard-Jones liquid: Statistics of stationary points," Physical Review Letters **85**, 5360 (2000).

[17] L. Angelani, G. Ruocco, M. Sampoli, and F. Sciortino, "General features of the energy landscape in Lennard-Jones-like model liquids," The Journal of Chemical Physics **119**, 2120 (2003).

[18] B. Doliwa and A. Heuer, "What does the potential energy landscape tell us about the dynamics of supercooled liquids and glasses?." Physical Review Letters **91**, 235501 (2003).

[19] F. Sciortino, "Potential energy landscape description of supercooled liquids and glasses," J. Stat. Mech., 050515(2005).

[20] A. Heuer, "Exploring the potential energy landscape of glass-forming systems: from inherent structures via metabasins to macroscopic transport," Journal of Physics: Condensed Matter **20**, 373101 (2008).

[21] G. Henkelman, B.P. Uberuaga, and H. Jónsson, "A climbing image nudged elastic band method for finding saddle points and minimum energy paths," The Journal of Chemical Physics **113**, 9901 (2000).

[22] G. Henkelman and H. Jónsson, "Improved tangent estimate in the nudged elastic band method for finding minimum energy paths and saddle points," The Journal of Chemical Physics **113**, 9978 (2000).

[23] P.G. Bolhuis, D. Chandler, C. Dellago, and P.L. Geissler, "Transition path sampling: Throwing ropes over rough mountain passes, in the dark," Ann. Rev. Phys. Chem. **53**, 291 (2002).

[24] G. Henkelman and H. Jónsson, "A dimer method for finding saddle points on high dimensional potential surfaces using only first derivatives," The Journal of Chemical Physics **111**, 7010 (1999).

[25] G. Henkelman, G. Jóhannesson, and H. Jónsson, "Methods for finding saddle points and minimum energy paths," in *Prog. Theor. Chem. and Phys.*, edited by S. D. Schwartz (Kluwer Academic, 2000).

[26] L.J. Munro and D.J. Wales, "Defect migration in crystalline silicon," Physical Review B **59**, 3969 (1999).

[27] R. Malek and N. Mousseau, "Dynamics of Lennard-Jones clusters: A characterization of the activation-relaxation technique," Physical Review E **62**, 7723 (2000).

[28] B. Doliwa and A. Heuer, "Energy barriers and activated dynamics in a supercooled Lennard-Jones liquid," Physical Review E **67**, 031506 (2003).

[29] J.P.K Doye and D.J. Wales, "Saddle points and dynamics of Lennard-Jones clusters, solids, and supercooled liquids," The Journal of Chemical Physics **116**, 3777 (2002).

[30] A. Pedersen and M. Luiser, "Bowl breakout: Escaping the positive region when searching for saddle points," The Journal of Chemical Physics **141**, 024109 (2014).

[31] A. Laio and M. Parrinello, "Escaping free-energy minima," Proceedings of the National Academy of Sciences (USA) **99**, 12562 (2002).

[32] J.P.K. Doye and D.J. Wales, "Comment on quasisaddles as relevant points of the potential energy surface in the dynamics of supercooled liquids[J. Chem. Phys. 116, 10297 (2002)]," The Journal of Chemical Physics **118**, 5263 (2003).

[33] L. Angelani, R. Di Leonardo, G. Ruocco, A. Scala, and F. Sciortino, "Quasisaddles as relevant points of the potential energy surface in the dynamics of supercooled liquids," The Journal of Chemical Physics **116**, 10297 (2002).

[34] J. Duncan, Q. Wu, K. Promislow, and G. Henkelman, "Biased gradient squared descent saddle point finding method," The Journal of Chemical Physics **140**, 194102 (2014).

[35] S. Bonfanti, *Low Temperature Theoretical and Numerical Study of Structural Glasses*, Ph.D. thesis, Università degli Studi dell'Insubria and University of Montpellier (2016).

[36] K. Müller and L. D. Brown, "Location of saddle points and minimum energy paths by a constrained simplex optimization procedure," Theoretica Chimica Acta **53**, 75 (1979).

[37] K. Ruedenberg and J.Q. Sun, "Gradient fields of potential energy surfaces," The Journal of Chemical Physics **100**, 5836 (1994).

[38] D. Passerone and M. Parrinello, "Action-derived molecular dynamics in the study of rare events," Physical Review Letters **87**, 108302 (2001).